

Quark-Gluon Plasma Fireball

Salah Hamieh, Jean Letessier and Johann Rafelski*

Department of Physics, University of Arizona, Tucson, AZ 85721

and

*Laboratoire de Physique Théorique et Hautes Energies***

Université Paris 7, 2 place Jussieu, F-75251 Cedex 05.

(June 7, 2000; July 4, 2000)

Lattice-QCD results provide an opportunity to model, and extrapolate to finite baryon density, the properties of the quark-gluon plasma (QGP). Upon fixing the scale of the thermal coupling constant and vacuum energy to the lattice data, the properties of resulting QGP equations of state (EoS) are developed. We show that the physical properties of the dense matter fireball formed in heavy ion collision experiments at CERN-SPS are well described by the QGP-EoS we presented. We also estimate the properties of the fireball formed in early stages of nuclear collision, and argue that QGP formation must be expected down to 40A GeV in central Pb-Pb interactions.

PACS: 12.38.Mh, 12.40.Ee, 25.75.-q

I. INTRODUCTION

It is believed today that a new state of matter has been formed in relativistic nuclear collisions at CERN [1]. The existence of a novel non-nuclear high temperature phase of elementary hadron matter, consisting of deconfined quarks and gluons, arises from the current knowledge about quantum chromodynamics (QCD), the theory of strong interaction. At sufficiently high temperature, the strong interactions weaken (asymptotic freedom), and thus we expect that hot and dense nuclear matter will behave akin to a free gas of quarks and gluons [2]. At issue is today if the new phase of matter observed at CERN is indeed this so called quark-gluon plasma (QGP) phase. One of the ways to test, and possibly falsify, the QGP hypothesis is to consider if the expected properties of the QGP indeed agree with experimental data which have been at the center of the CERN announcement.

The observational output of experiments we consider are particle abundances and particle spectra. We address here results on hadron and strange hadron production at the equivalent center of momentum reaction energy $E_{\text{CM}} = 8.6$ GeV per baryon in Pb-Pb reactions. As seen in many experimental results [1], which we will not restate here in further detail, in these high energy nuclear collisions a localized dense and hot matter fireball is formed. In our earlier analysis of experimental results [3,4], we have obtained diverse physical properties of the source, such as energy per baryon content E/b , entropy per baryon content S/b , and last, not least, strangeness content per baryon \bar{s}/b . These values are associated with temperature T_f and baryo-chemical potential μ_b at which these hadron abundances are produced (chemical freeze out), along with other chemical properties and the collective velocity of the matter emitting these particles v_c .

Our main aim is thus to compare the properties of the QGP phase, modeled to agree with the lattice-QCD calculations [6], to the properties of the fireball obtained

in the study of hadronic particle abundances. We thus develop semi-phenomenological QGP equations of state (EoS) based on thermal and lattice-QCD results. These are then applied to explore, in a systematic fashion, properties of the fireball formed in the Pb-Pb reactions. We show that the physical properties of the fireball extracted from particle production data are the same as obtained employing our QGP-EoS.

Using our QGP-EoS we also explore the initial thermal conditions reached in the collision both in, and out, of quark chemical equilibrium. We have already shown previously that the strangeness yield is following the predicted QGP yield [3,4]. We also show that, when the energy and baryon number deposited in the initial fireball drops below 20%, *e.g.* due to large impact parameter interactions, or/and small nuclei involved in the collision, the formation of the QGP phase becomes improbable.

An important dynamical aspect of our experimental data analysis [3,4], on which this work relies, is the sudden disintegration (hadronization) of the fireball into the final state hadrons. This reaction mechanism is *a priori* not very surprising, since a fireball formed in these collisions explodes, driven by internal compression pressure. However, we did not see in the particle production analysis a generally expected signature of an ensuing, confined hadron phase. Moreover, the particle production temperature (chemical freeze-out) we found corresponds to a deeply super-cooled state, which can be subject to mechanical instability [7]. We have checked elsewhere this assertion, applying the EoS developed here in a detailed analysis of the fireball sudden break-up, and have found that it occurs at the condition of mechanical instability [8].

A consequence of the sudden fireball break up is that akin to the situation found in the study of properties of the early universe, particle abundances do not reach chemical equilibrium. Our analysis accounts in full for this important fact [3,5]. For an appropriate criticism of the chemical equilibrium models, and a list of related

work, we refer the reader to work of Biró [9].

In the next section, we address the thermal QCD interaction coupling α_s we will use. In section III, we define the equations of state and the parameters of our approach and explore which is the best scheme for the extrapolation of the lattice data. In section IV, we present properties of the QGP phase, relevant both to the study of the freeze-out conditions, and the study of the initial conditions reached in the collision. We present and discuss the comparison of the properties of the exploding fireball with those measured by means of hadron production in section V. Our conclusions follow in section VI.

II. QCD INTERACTIONS IN PLASMA

The energy domain in which we explore diverse properties of dense strongly interacting matter is barely above the scale 1 GeV and thus, in our consideration, an important input is the scale μ dependence of the QCD coupling constant, $\alpha_s(\mu)$, which we obtain solving

$$\mu \frac{\partial \alpha_s}{\partial \mu} = -b_0 \alpha_s^2 - b_1 \alpha_s^3 + \dots \equiv \beta_2^{\text{pert}}. \quad (1)$$

β_2^{pert} is the beta-function of the renormalization group in two loop approximation, and

$$b_0 = \frac{11 - 2n_f/3}{2\pi}, \quad b_1 = \frac{51 - 19n_f/3}{4\pi^2}.$$

β_2^{pert} does not depend on the renormalization scheme, and solutions of Eq. (1) differ from higher order renormalization scheme dependent results by less than the error introduced by the experimental uncertainty in the measured value of $\alpha_s(\mu = M_Z) = 0.118 + 0.001 - 0.0016$. When solving Eq. (1) with this initial condition, we cross several flavor mass thresholds and thus $n_f(\mu)$ is not a constant in the interval $\mu \in (1, 100)$ GeV. Any error made when not properly accounting for n_f dependence on μ accumulates in the solution of Eq. (1). In consequence, a popular approximate analytic solution shown as function of T , as dotted line in figure 1,

$$\alpha_s(\mu) \simeq \frac{2}{b_0 \bar{L}} \left[1 - \frac{2b_1}{b_0^2} \frac{\ln \bar{L}}{\bar{L}} \right], \quad \bar{L} \equiv \ln(\mu^2/\Lambda^2), \quad (2)$$

with $\Lambda = 0.15$ GeV and $n_f = 3$, is not precise enough compared to the exact 2-loop numerical solution.

We show the numerical solution for $\alpha_s(\mu)$ in figure 1, setting

$$\mu = 2\pi T = \kappa T/T_c, \quad \kappa = 1 \text{ GeV}.$$

where the solid line corresponds to $\alpha_s(\mu = M_Z) = 0.118$, bounded by the experimental uncertainty [10]. We observe that the expansion parameter of thermal QCD is relatively small, $\alpha_s/\pi < 0.25$, which makes the following discussion possible. The difference between the dotted

line and the exact result, in figure 1, is very relevant and has been at the origin of considerable confusion regarding the behavior of the interacting hot quark-gluon gas [11]. Since the lattice work chooses the value of T_c to match the string tension, use of false α_s is physically inconsistent.

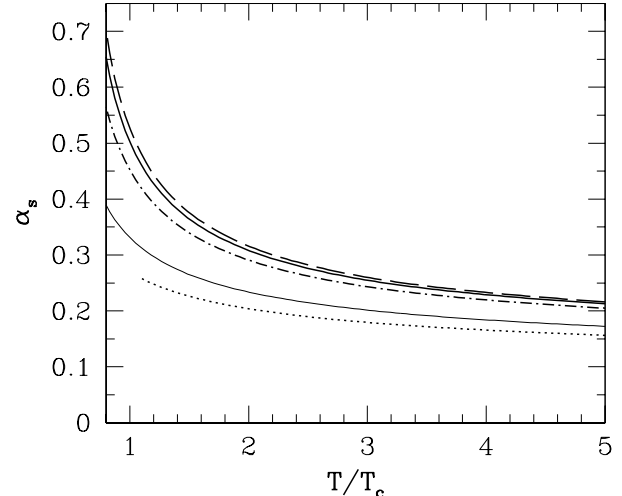


FIG. 1. $\alpha_s(2\pi T)$ for $T_c = 0.16$ GeV. Dashed line: $\alpha_s(M_Z) = 0.119$; solid line = 0.118; dot-dashed line = 0.1156. Dotted line: approximate 2-loop solution given in Eq.(2). Thin solid line: same as dotted, but extrapolating with $n_f = 5$ to $\alpha_s(M_Z) = 0.118$.

We stress that the analytical function, Eq. (2), is in fact a very good solution of Eq. (1). For $\Lambda = 0.225$ GeV and $n_f = 5$, it agrees with numerical result for the entire range, $M_Z = 92$ GeV $> \mu > M_B \simeq 4.5$ GeV, in which $n_f = \text{Const.}$, here M_B is the bottom quark mass. However, these were not the parameters considered in the thermal QCD work [12–15], and, moreover, the region of interest for the QGP equations of state we explore is $1 \text{ GeV} < \mu < M_B$, where n_f varies. The thin solid line, in figure 1, shows the behavior of the analytical solution with $n_f = 5$ kept constant, and for $\Lambda = 0.225$ GeV which assures the boundary value $\alpha_s(M_Z) = 0.118$.

III. THE QUARK-GLUON LIQUID

We now can define the quark-gluon liquid model which describes well the properties of QGP determined by lattice-QCD method.

1. To relate the QCD scale to the temperature $T = 1/\beta$, we use for the scale [16]:

$$\mu = 2\pi\beta^{-1} \sqrt{1 + \frac{1}{\pi^2} \ln^2 \lambda_q} = 2\sqrt{(\pi T)^2 + \mu_q^2}. \quad (3)$$

This extension to finite chemical potential μ_q , or equivalently quark fugacity $\lambda_q = \exp \mu_q/T$, is motivated by the form of plasma frequency entering the computation of the vacuum polarization function [17]. In principle,

there should be in Eq. (3) also a contribution from the strange quark chemical fugacity λ_s expressed equivalently by the strange quark chemical potential μ_s . However since strangeness conservation virtually assures that $\mu_s \simeq 0$, or equivalently, $\lambda_s \simeq 1$, we will not pursue this further.

2. To reproduce the lattice results available at $\mu_q = 0$ [6], we need to introduce, in the domain of freely mobile quarks and gluons, a finite vacuum energy density [11]:

$$\mathcal{B} = 0.19 \frac{\text{GeV}}{\text{fm}^3}.$$

This also implies, by virtue of relativistic invariance, that there must be a (negative) associated pressure acting on the surface of this volume, aiming to reduce the size of the deconfined region. These two properties of the vacuum follow consistently from the vacuum partition function:

$$\ln \mathcal{Z}_{\text{vac}} \equiv -\mathcal{B}V\beta. \quad (4)$$

3. The partition function of the quark-gluon liquid comprises interacting gluons, n_q flavors of light quarks [18], and the vacuum \mathcal{B} -term. We incorporate further the strange quarks by assuming that their mass in effect reduces their effective number $n_s < 1$:

$$\begin{aligned} \frac{T}{V} \ln \mathcal{Z}_{\text{QGP}} \equiv P_{\text{QGP}} &= -\mathcal{B} + \frac{8}{45\pi^2} c_1 (\pi T)^4 \\ &+ \frac{n_q}{15\pi^2} \left[\frac{7}{4} c_2 (\pi T)^4 + \frac{15}{2} c_3 \left(\mu_q^2 (\pi T)^2 + \frac{1}{2} \mu_q^4 \right) \right] \\ &+ \frac{n_s}{15\pi^2} \left[\frac{7}{4} c_2 (\pi T)^4 + \frac{15}{2} c_3 \left(\mu_s^2 (\pi T)^2 + \frac{1}{2} \mu_s^4 \right) \right], \end{aligned} \quad (5)$$

where:

$$\begin{aligned} c_1 &= 1 - \frac{15\alpha_s}{4\pi} + \dots, \\ c_2 &= 1 - \frac{50\alpha_s}{21\pi} + \dots, \quad c_3 = 1 - \frac{2\alpha_s}{\pi} + \dots. \end{aligned} \quad (6)$$

In figure 2, the ‘experimental’ values are from numerical lattice simulations of P/T^4 [6]. For practical reasons the lattice results for ‘massless’ 2 and 3-flavors were obtained with $m/T = 0.4$, which reduces the particle numbers by 2%, and this effect is allowed for in the quark-gluon liquid lines (two flavors: dashed, three flavors: dotted) in figure 2. In the case 2+1 flavors, a renormalized strange quark mass $m_s/T = 1.7$, the lattice input has been $m_s^0/T = 1$. This leads to a $\simeq 50\%$ reduction in strange quark number, thus $n_s \simeq 0.5$ will be used in our study of QGP properties, assuming that strangeness is fully chemically equilibrated, unless otherwise noted. Thus, in general, we have $n_f = n_q + n_s \simeq 2.5$.

The thin lines, in figure 2, correspond to the previously reported results for a quark-gluon gas [15], with first order QCD correction introduced using an approximate value of $\alpha_s(\mu)$, Eq. (2), and without the vacuum pressure term. For $T \geq 2T_c$, the disagreement is an artifact of the approximation used for α_s .

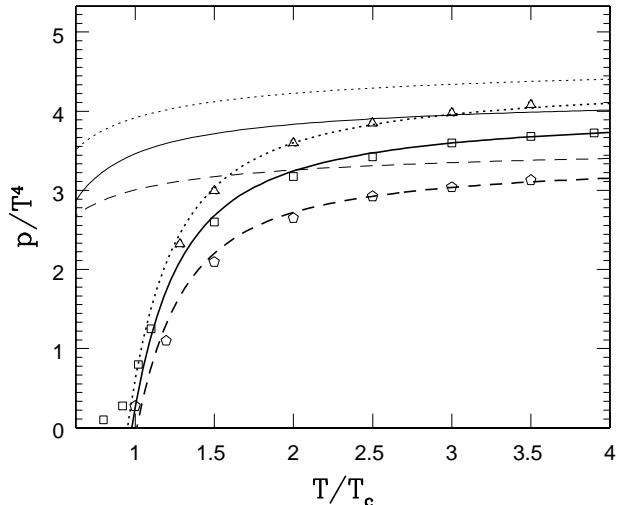


FIG. 2. Lattice-QCD results [6] for P/T^4 at $\lambda_q = 1$, compared with our quark-gluon liquid model (thick lines) and lowest order perturbative QCD using approximate α_s , Eq. (2) (thin lines used in prior work [12–15]);: dotted line 3 flavors, solid line 2+1 flavors, and dashed line 2 flavors.

Lattice results were also informally reported [1] for the energy density with $n_f = 3$, and are shown in figure 3, upper ‘experimental’ points. The energy density,

$$\epsilon_{\text{QGP}} = -\frac{\partial \ln \mathcal{Z}_{\text{QGP}}(\beta, \lambda)}{V \partial \beta}, \quad (7)$$

is sensitive to the slope of the partition function. We show, in figure 3, the energy density and pressure for two extreme theoretical approaches: the solid lines are for the model we described above ($\mu = 2\pi T$, $\mathcal{B} = 0.19 \text{ GeV}/\text{fm}^3$), the dotted lines are obtained in the thermal expansion, including all, up to fifth order, scale dependent terms obtained by Zhai and Kastening [13], and choosing the scale $\mu = 2.6\pi T$ in free energy and in the coupling constant, so the result reproduces the pressure well (bottom dotted line in figure 3).

In the upper portion of figure 3, comparing these two theoretical approaches chosen to reproduce the pressure, we see a clear difference in the energy density. The 5th order energy density (dotted line) $(g/4\pi)^5 = (\alpha_s/\pi)^{5/2}/32$ [13], disagrees with the lattice data also at high T , where these are most precise. Near to $T \simeq 1.5T_c$, the solid line is visibly better describing the pressure. In fact, systematic study of the behavior of the $(g/4\pi)^n$ expansion reveals that higher order terms do not appear to lead to a convergent result for the range of temperatures of interest to us [13,15].

It is not uncommon to encounter in a perturbative expansion a semi-convergent series. The issue then is how to establish a workable scheme. Our result implies that the choice of the Matsubara frequency $2\pi T$ as the scale μ of the running coupling constant has for yet unknown reasons, the effect to minimize the contribution of the sum of all higher order terms in the expansion, even for

moderate temperatures, once the vacuum pressure is introduced.

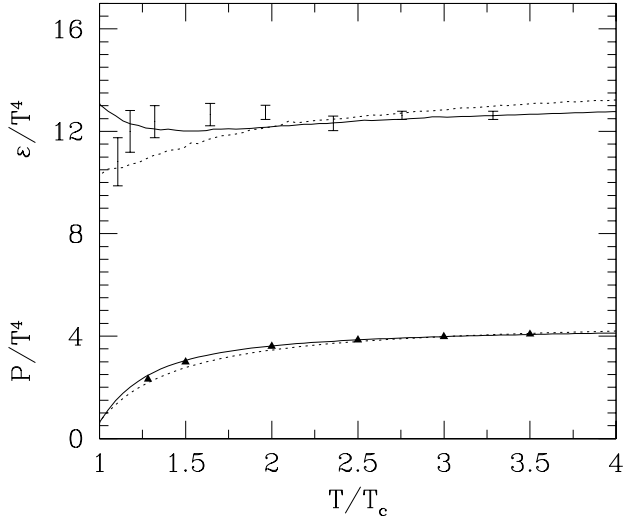


FIG. 3. Top: informal lattice-QCD results [1] for ε/T^4 at $\lambda_q = 1$, compared with our quark-gluon liquid model (solid line). Dotted line is an alternative approach in which all terms in partition function are summed as given in [13] and the scale is set at $\mu = 2.6\pi T$. Bottom: published lattice pressure results [6] compared to the two approaches. Solid line: first order with the bag constant; dotted line: 5th order with $\mu = 2.6\pi T$.

Aside of the theoretical elegance of using the Matsubara frequency as the scale when employing lowest order thermal perturbation theory, the fact that this very simple approach adequately describes both pressure and energy density supports our belief that we have found an appropriate extrapolation of the QGP properties to finite baryon density. However, we could not test if the coefficient c_3 , Eq. (6), describes well the behavior of the partition function for finite chemical potentials, as such lattice-QCD results are not available. By using this term, we rely on the expansion in α_s as implied by Eq. (5). This, in fact, is a practical reason for us to prefer the simpler (1st order in α_s) approach, since the expansion of Zhai and Kastening [13] was computed in the limit of vanishing chemical potential.

The quantities we show, in figure 2 and figure 3, are all divided by a large factor, T^4 , in order to make the small differences between lattice results and thermal theory visible. In absolute terms, the model we now adopt for further study reproduces the lattice results well, at the level of a few percent. It can only be hoped that the lattice results have reached that level of precision. In our approach, the value of \mathcal{B} we obtain and employ is entirely dependent on the quality of the lattice results. However, in another work [8], we have considered the dynamics of the expanding fireball and obtained an estimate for the value of \mathcal{B} as defined here. We found that $\mathcal{B} \geq 0.17 \text{ GeV/fm}^3$, consistent with the value we employ here $\mathcal{B} = 0.19 \text{ GeV/fm}^3$.

IV. PROPERTIES OF QGP-LIQUID

We are now ready to explore the physical properties of the quark-gluon liquid. The energy density is obtained from Eq. (5), recalling that the scale of the interaction is given by Eq. (3):

$$\epsilon_{\text{QGP}} = 4\mathcal{B} + 3P_{\text{QGP}} + A_g + A_q + A_s, \quad (8)$$

$$A_g = (b_0\alpha_s^2 + b_1\alpha_s^3) \frac{2\pi}{3} T^4, \quad (9)$$

$$A_q = (b_0\alpha_s^2 + b_1\alpha_s^3) \left[\frac{5\pi n_q}{18} T^4 + \frac{n_q}{\pi} \left(\mu_q^2 T^2 + \frac{\mu_q^4}{2\pi^2} \right) \right], \quad (10)$$

$$A_s = (b_0\alpha_s^2 + b_1\alpha_s^3) \left[\frac{5\pi n_s}{18} T^4 + \frac{n_s}{\pi} \left(\mu_s^2 T^2 + \frac{\mu_s^4}{2\pi^2} \right) \right]. \quad (11)$$

A convenient way to obtain entropy and baryon density uses the thermodynamic potential \mathcal{F} :

$$\frac{\mathcal{F}(T, \mu_q, V)}{V} = -\frac{T}{V} \ln \mathcal{Z}(\beta, \lambda_q, V)_{\text{QGP}} = -P_{\text{QGP}}. \quad (12)$$

The entropy density is:

$$s_{\text{QGP}} = -\frac{d\mathcal{F}}{VdT}, \quad (13)$$

$$= \frac{(n_q + n_s)7\pi^2}{15} c_2 T^3 + n_q c_3 \mu_q^2 T + n_s c_3 \mu_s^2 T + \frac{32\pi^2}{45} c_1 T^3 + (A_g + A_q + A_s) \frac{\pi^2 T}{\pi^2 T^2 + \mu_q^2}. \quad (14)$$

Noting that baryon density is $1/3$ of quark density, we have:

$$\rho_b = -\frac{1}{3} \frac{d\mathcal{F}}{Vd\mu_q} \quad (15)$$

$$= \frac{n_q}{3} c_3 \left\{ \mu_q T^2 + \frac{1}{\pi^2} \mu_q^3 \right\} + \frac{n_s}{3} c_3 \left\{ \mu_s T^2 + \frac{1}{\pi^2} \mu_s^3 \right\} + \frac{1}{3} (A_g + A_q + A_s) \frac{\mu_q}{\pi^2 T^2 + \mu_q^2}. \quad (16)$$

We show properties of the quark-gluon liquid in a wider range of parameters in figure 4. We study the properties at fixed entropy per baryon S/b since an isolated ideal particle fireball would evolve at a fixed S/b . We consider the range $S/b = 10$ (at left for the top panel, baryochemical potential μ_b , and middle panel baryon density n/n_0 , here $n_0 = 0.16/\text{fm}^3$, and bottom left for the energy per baryon E/b) in step of 5 units, up to maximum of $S/b = 60$. The highlighted curve, in figure 4, is for the value $S/b = 42.5$, which value follows from earlier study of hadronic particle spectra [3]. The dotted line, at the minimum of $E/b|_{S/b}$, is where the vacuum and quark-gluon gas pressure balance. This is the equilibrium point and indeed the energy per baryon does have a relative minimum there.

Unlike the case for an ideal quark-gluon gas, the lines of fixed S/b , seen in the top panel of figure 4 are not corresponding to $\mu_b/T = \text{Const.}$, though for large T and small

μ_b they do show this asymptotic behavior. Since little entropy is produced during the evolution of the QGP fireball, the thick line in the lower panel of figure 4 describes the approximate trajectory in time of the fireball made in Pb-Pb interactions at the projectile energy 158A GeV. We stress that there has been no adjustment made in any parameter to bring the earlier determined ‘experimental’ points shown in figure 4 into the remarkable agreement with the properties of equations of state of the quark-gluon plasma. The same embarrassing agreement is seen in figure 5.

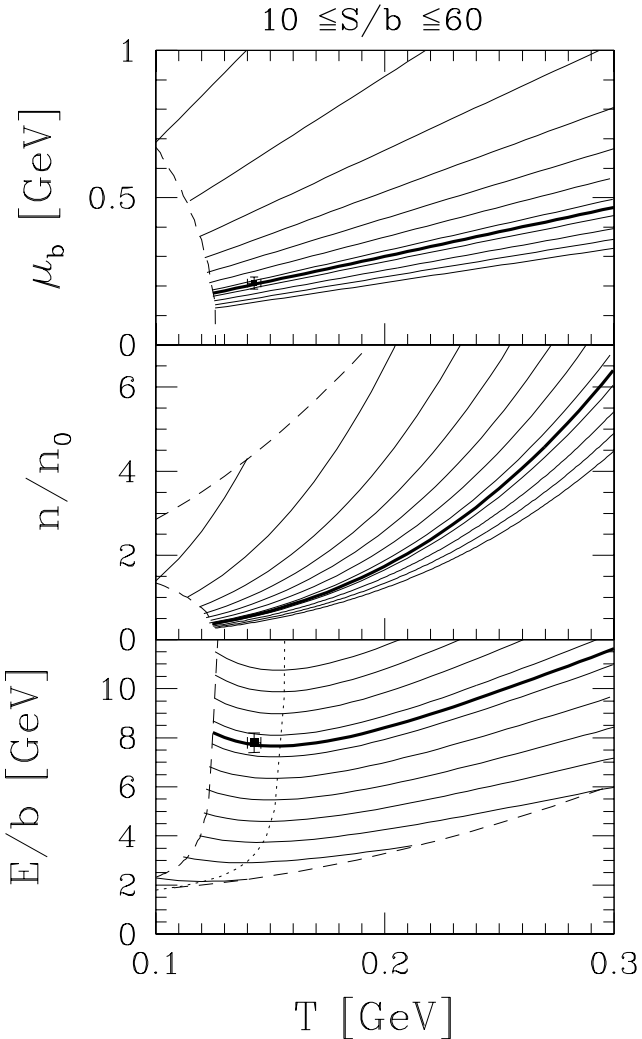


FIG. 4. From top to bottom: μ_b , n/n_0 and E/b ; lines shown correspond to fixed entropy per baryon $S/b = 10$ to 60 by step of 5 (left to right). Thick solid lines: result for $S/b = 42.5$. Limits: energy density $\varepsilon_{q,g} = 0.5 \text{ GeV/fm}^3$ and baryo-chemical potential $\mu_b = 1 \text{ GeV}$. The experimental points denote chemical freeze-out analysis result [3], discussed in section V.

The trajectories at fixed energy per baryon E/b are shown in the $T-\lambda_q$ plane in figure 5, for the values (beginning at right) $E/b = 2.5$ to 9.5 GeV by step

of 1. The highlighted curve corresponds to the value $E/b = 7.8 \text{ GeV}$ which is the local intrinsic energy content of the hadronizing QGP fireball formed at SPS Pb-Pb interactions at the projectile energy 158A GeV [3]. Dotted line, in figure 5, corresponds to $P = 0$, the solid line that follows it is the phase transition line where the QGP pressure is balanced by pressure of the hadron gas. This is the condition at which the equilibrium transition would occur in a slowly evolving system, such as would be the early universe. The properties of hadronic gas are obtained resuming numerically the contribution of all known hadronic particles including resonances, which effectively accounts for the presence of interactions in the confined hadron gas phase [19].

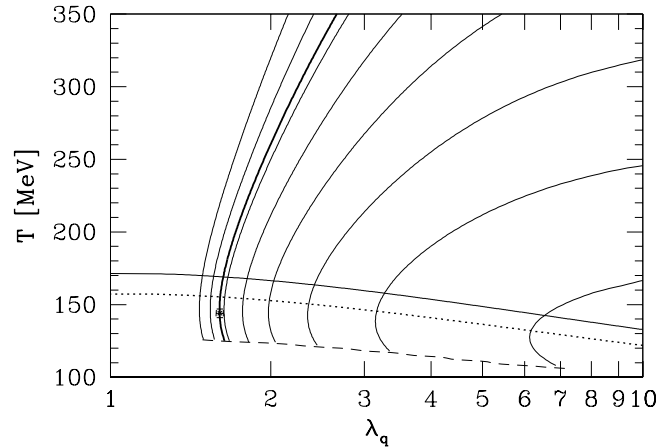


FIG. 5. Contours of constant energy per baryon in QGP in the $T-\lambda_q$ plane: From right to left $E/b = 2.5$ to 9.5 GeV by step of 1, thick solid line is for $E/b = 7.8 \text{ GeV}$. Dotted line corresponds to $P = 0$, above this, the solid line is the phase transition where the QGP pressure is balanced by pressure of the hadron gas. The experimental point denotes chemical freeze-out analysis result [3], see section V. Bottom dashed line boundary is at energy density 0.5 GeV/fm^3 .

In relativistic nuclear collisions, the formation of equilibrium state competes with the evolution of the fireball. The slowest of all the equilibria is certainly the chemical equilibration of strange quarks [20]. Next slowest is the equilibration of light quarks. The chemical relaxation time constant for the production of light quarks has been obtained in the first consideration of chemical QGP equilibration, see figure 2 in [20]: $\tau_{GG \rightarrow q\bar{q}}(T = 250 \text{ MeV}) = 0.3 \text{ fm}$. The chemical equilibration of gluons has also been questioned, and is found to be slow, when only $2G \rightarrow 3G$ processes are allowed [21]. Since gluon fusion processes are proportional to the square of gluon abundance, $\tau_{GG \rightarrow q\bar{q}}(T = 250 \text{ MeV}) \rightarrow 1.2 \text{ fm}$ for processes occurring when gluons are at 50% of equilibrium abundance. This explains why quarks trail gluons in the approach to equilibrium, which are struggling to equilibrate by multi-gluon production processes [22]. It is generally assumed that the approximate thermal (ki-

netic) equilibrium is established much faster. The mechanisms of this process remain under investigation [23].

In figure 6, a case study how the chemical equilibration of quarks cools the gluon-chemically equilibrated fireball is presented. The change of both the initial temperature T_i (upper panel) and λ_q (lower panel) as function of n_f , for $E/b = 9.3$ GeV, the total final energy content of Pb-Pb collisions at CERN, is presented. We see that in the initial state an equilibrated glue phase at $T \simeq 270$ MeV may have been reached. Full chemical equilibrium would correspond to $T \geq 230$ MeV, but more likely this value is somewhat reduced due to flow dilution that has occurred in the process of chemical equilibration.

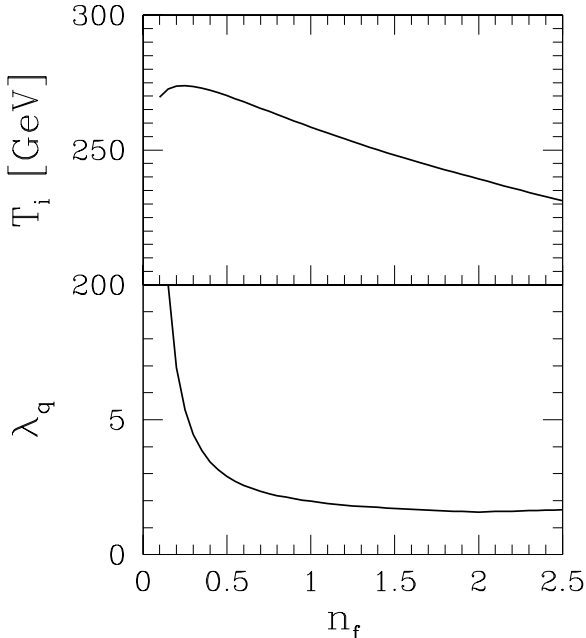


FIG. 6. The initial conditions as function of the number of Fermi degrees of freedom n_f . Upper panel for temperature and lower for quark fugacity, at $E/b = 9.3$ GeV.

One of the interesting quantities is the QGP energy density which we show in figure 7, for both fixed E/b (top) and fixed S/b bottom, for fully equilibrated condition $n_q = 2, n_s = 0.5$. We see that for $E/b > 6$ GeV and $S/b > 25$ the influence of finite baryo-chemical potential is minimal and the lines coalesce. In other words, at conditions we encounter at SPS, we can correlate the energy density with temperature alone $\varepsilon \simeq aT^4$, as seen for $n_f = 3 > 2.5$ in figure 3. In figure 7, we see that the energy density $3 \text{ GeV}/\text{fm}^3$ is established when the temperature in the equilibrated fireball equals 212 MeV. Considering the observed high inverse slopes of strange particles, one can assume that the the plasma phase, before it reached full chemical equilibrium, has been at about $T \simeq 250$ MeV and the energy density in this state has most likely been still higher, above $4 \text{ GeV}/\text{fm}^3$. We believe that our evaluation of the properties of the QGP liquid is, at this range of temperature $T \simeq 1.5T_c$, reliable.

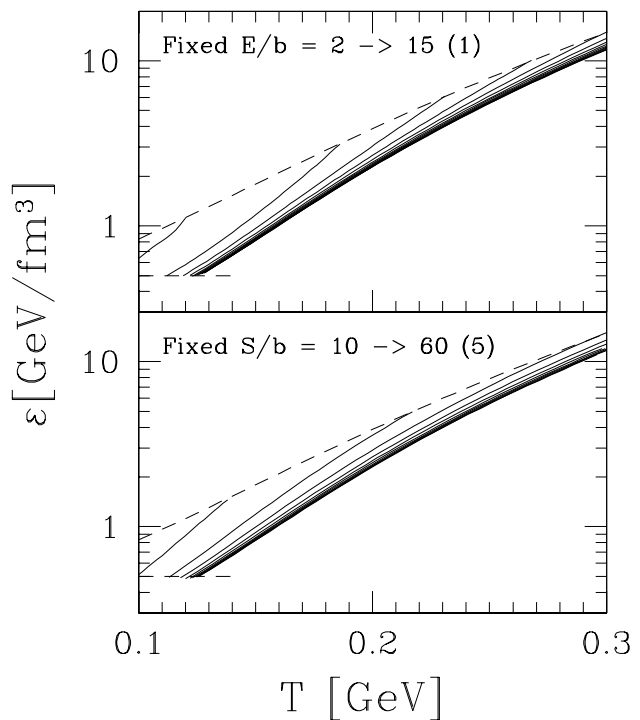


FIG. 7. Energy density in QGP as function of temperature. Top panel: for a fixed Energy per baryon $E/b = 2$ to 15 GeV by step of 1; bottom panel for fixed entropy per baryon $S/b = 10$ to 60 by step of 5. Boundaries are $\varepsilon = 0.5 \text{ GeV}/\text{fm}^3$ at the bottom and $\mu_b = 1 \text{ GeV}$ at the top.

As a final step in the study of the properties of the QGP liquid, we consider the conditions relevant for the formation of the QGP, and consider the behavior for $n_f = 1$. We show, in figure 8, lines of fixed energy per baryon $E/b = 3, 4, 5, 6, 8, 10, 20, 50$ and 100 GeV, akin to results we have shown for $n_f = 2 + 0.5$, in figure 5. The horizontal solid line is where the equilibrated hadronic gas phase has the same pressure as QGP-liquid with semi-equilibrated quark abundance. The free energy of the QGP liquid must be lower (pressure higher) in order for hadrons to dissolve into the plasma phase. The dotted lines in figure 5, from bottom to top, show where the pressure of the semi-equilibrated QGP phase is equal to $\eta = 20\%, 40\%, 60\%, 80\%$ and 100% , η being the ‘stopping’ fraction of the dynamical collisional pressure [24]:

$$P_{\text{col}} = \eta \rho_0 \frac{P_{\text{CM}}^2}{E_{\text{CM}}}.$$

The rationale to study, in figure 8, lines at fixed E/b is that, during the nuclear collision which lasts about $2R_N/\gamma_L 2c \simeq 13/18 \text{ fm}/c$, where γ_L is the Lorentz factor between the lab and CM frame and R_N is the nuclear radius, parton collisions lead to a partial (assumed here to be 1/2) chemical equilibration of the hadron matter. At that time, the pressure exercised corresponds to collisional pressure P_{col} . This stopping fraction, seen in the transverse energy produced, is about 40% for S-S

collisions at $200A$ GeV and 60% for Pb–Pb collisions at $158A$ GeV. If the momentum-energy and baryon number stopping are similar, as we see in the experimental data, then the SPS collisions at 160 – $200A$ GeV are found in the highlighted area left of center of the figure. In the middle of upper boundary of this area, we would expect the beginning evolution of the thermal but not yet chemically equilibrated Pb–Pb fireball, and in the lower left corner of the S–S fireball. We note that the temperature reached in S–S case is seen to be about 25 MeV lower than in the Pb–Pb case. The lowest dotted line (20% stopping) nearly coincides with the non-equilibrium phase boundary (solid horizontal line, in figure 8) and thus we conclude that this is, for the condition $n_f = 1$, the lowest stopping that can lead to formation of a deconfined QGP phase. Such a low stopping would be encountered possibly in lighter than S–S collision systems or/and at large impact parameter interactions of larger nuclei.

The highlighted area, right of center of the figure 8, corresponds to the expected conditions in Pb–Pb collisions at $40A$ GeV. If we assume that the stopping here is near 80%, then the initial conditions for fireball evolution would be found towards the upper right corner of this highlighted area. We recognize that the higher stopping nearly completely compensates the effect of reduced available energy in the collision and indeed, we expect that we form QGP also at these collision energies. It is important to realize that we are entering a domain of parameters, in particular λ_q , for which the extrapolation of the lattice results is not necessarily reliable, and thus our equations of state have some systematic uncertainty.

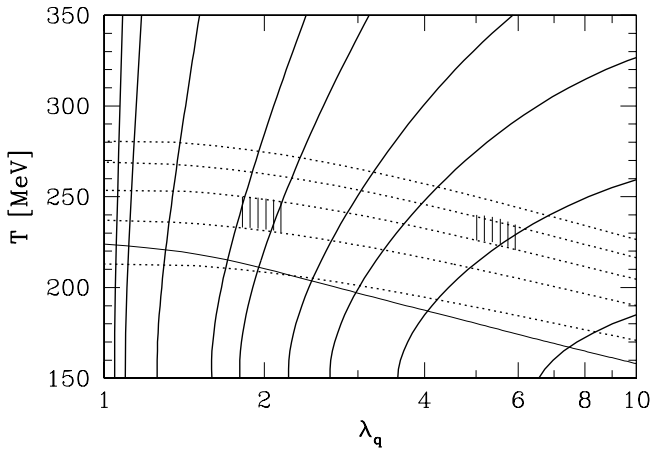


FIG. 8. Contours of energy per baryon in QGP in the T – λ_q plane for $n_f = 1$: From right to left $E/b = 3, 4, 5, 6, 8, 10, 20, 50$ and 100 GeV. Thin, nearly horizontal line: hadronic gas phase has the same pressure as the QGP-liquid with semi-equilibrated quark flavor. Dotted lines from bottom to top: pressure in QGP liquid equals 20%, 40%, 60%, 80%, and 100%, of the dynamical collisional pressure

V. EXPERIMENTAL DATA ANALYSIS AND QGP-EOS

A full account of our prior analysis of the $158A$ GeV Pb–Pb collision system has appeared [3,4]. We briefly summarize the results that we require for the study of QGP properties at fireball breakup. In table I, in upper section, we present the parameters T_f (the chemical freeze-out temperature), v_c (the collective flow velocity at sudden breakup), λ_q (the light quark fugacity), λ_s (the strange quark fugacity), γ_q (the light quark phase space occupancy), γ_s (the strange quark phase space occupancy). These are derived from analysis of all hadrons excluding Ω and $\bar{\Omega}$, which data points are not following the same systematic production pattern. These parameters characterize completely the physical properties of the produced hadrons, and these properties are shown in the bottom section of table I.

In the heading of the table, the total error, χ^2 is shown, along with the number of data points N , parameters p and data point constraints r . The confidence level that is reached in our description is near or above 90%, depending on scenario considered. The scenarios we consider are seen in the columns of table I: an unconstrained description of all data in the first column, constraint to exact strangeness conservation in the observed hadrons, second column. Since in both cases the parameter γ_q assumes value that maximizes the entropy and energy content in the pion gas, we assume this value in the so constrained third column.

TABLE I. Results of study of Pb–Pb hadron production [3]: in the heading: the total quadratic relative error χ^2_T , number of data points N , parameters p and redundancies r ; in the upper section: statistical model parameters which best describe the experimental results for Pb–Pb data. Bottom section: specific energy, entropy, anti-strangeness, net strangeness of the full hadron phase space characterized by these statistical parameters. In column one, all statistical parameters and the flow vary. In column two we fix λ_s by requirement of strangeness conservation, and in column three, we fix γ_q at the pion condensation point $\gamma_q = \gamma_q^c$.

| $\chi^2_T; N; p; r$ | $\text{Pb} _v$ | | |
|-----------------------|----------------------------|----------------------------|----------------------------------|
| | $\text{Pb} _v^{\text{sb}}$ | $\text{Pb} _v^{\text{sc}}$ | |
| T_f [MeV] | 142 ± 3 | 144 ± 2 | 142 ± 2 |
| v_c | 0.54 ± 0.04 | 0.54 ± 0.025 | 0.54 ± 0.025 |
| λ_q | 1.61 ± 0.02 | 1.605 ± 0.025 | 1.615 ± 0.025 |
| λ_s | 1.09 ± 0.02 | 1.10^* | 1.09 ± 0.02 |
| γ_q | 1.7 ± 0.5 | 1.8 ± 0.2 | $\gamma_q^{c*} = e^{m_\pi/2T_f}$ |
| γ_s/γ_q | 0.79 ± 0.05 | 0.80 ± 0.05 | 0.79 ± 0.05 |
| E_f/B | 7.8 ± 0.5 | 7.7 ± 0.5 | 7.8 ± 0.5 |
| S_f/B | 42 ± 3 | 41 ± 3 | 43 ± 3 |
| s_f/B | 0.69 ± 0.04 | 0.67 ± 0.05 | 0.70 ± 0.05 |
| $(\bar{s}_f - s_f)/B$ | 0.03 ± 0.04 | 0^* | 0.04 ± 0.05 |

We can now check the consistency between the statistical parameters (top panel of table I) and the physical properties of the fireball (bottom panel of table I) which are maintained in the process of hadronization. We note that the energy shown in this table, is the intrinsic energy in the flowing frame. The CM-laboratory energy includes the kinetic energy of the flow and thus is greater, to be obtained multiplying the result shown in table I by the Lorentz factor $\gamma = 1/\sqrt{1-v_c^2} = 1.19$. Thus the initial value of the energy per baryon that the system has had before expansion started has been $E^0/b \simeq 9.3 \text{ GeV}$, as used in figure 6 and in the estimate presented in figure 8.

In the bottom panel in figure 4, we saw that the Temperature $T_f = 143 \pm 3 \text{ MeV}$ and energy per baryon $E/b = 7.8 \text{ GeV}$ where just at $S/b = 42.5$ seen table I. Similarly, in the top panel, the baryo-chemical potential $\mu_b = 3T_f \ln \lambda_q = 204 \pm 10 \text{ MeV}$ is as required for the consistency of QGP properties. A similarly embarrassing agreement of the hadron yield analysis results with properties of the QGP fireball is seen in figure 5, but that is just a different representation (at fixed E/b) of the result we saw at fixed S/b , in figure 4. However, the importance of this result is that the plasma breakup point appears well below the phase transition temperature line (thin horizontal solid line). As this discussion shows, the properties of the QGP liquid at the point of hadronization are the same as found studying the properties of hadrons emerging from the exploding fireball. Both the specific energy and entropy content of the fireball are consistent with the statistical parameters T_f and μ_b according to our equations of state of the quark-gluon liquid. The freeze-out point at $T \simeq 143 \text{ MeV}$, seen in bottom panel of figure 4, corresponds to an energy density $\varepsilon_f \simeq 0.6 \text{ GeV/fm}^3$. This is the value for the super-cooled plasma, the equilibrium phase transition occurs at twice this value, $\varepsilon_p \simeq 1.3 \text{ GeV/fm}^3$.

We can also evaluate the hadronic phase space energy density. We need to introduce the excluded volume correction [25]. Considering that the point particle phase space energy density $\varepsilon_{pt} = 1.1 \text{ GeV/fm}^3$, we obtain $\varepsilon_{HG} \simeq 0.4 \text{ GeV/fm}^3$, using the value of $\mathcal{B} = 0.19 \text{ GeV/fm}^3$. Taking into account the numerous uncertainties in the understanding of the excluded volume effect, we conclude that the fireball energy density is comparable in magnitude to the energy density present in hadronic phase space. We also note that the equilibrium phase transition curve we had presented in figure 5 was computed without the excluded volume effect. When allowing for this, the solid line (critical curve) moves about half way towards the dotted line where $P_{QGP} = 0$.

For a vanishing baryo-chemical potential, $\lambda_q = 1$, we determine in figure 5, that the phase transition temperature for point hadrons is $T_p \simeq 172 \text{ MeV}$. The super-cooled $P = 0$ temperature is at $T_c = 157.5 \text{ MeV}$ (dotted line at $\lambda_q = 1$, in figure 5), and an expanding fireball can super-cool to as low as $T \simeq 145 \text{ MeV}$, where the mechanical instability occurs [7,8]. We also have seen this result in the bottom panel of figure 4 where the dotted

line, corresponding to pressure zero, is to the right of the ‘experimental’ point.

The collective velocity v_c of the exploding matter remains large in deeply super-cooled conditions even though the expansion slows down and kinetic energy is transferred back from flow to thermal component, once the dotted $P = 0$ line is crossed, as can be seen in figure 4. Interestingly, our central value $v_c = 0.54$ is the velocity of sound of the exploding fireball:

$$v_s^2 = \left. \frac{\partial P}{\partial \varepsilon} \right|_{S/b} . \quad (17)$$

The theoretical line shown in figure 9 is computed for $S/b = 42$.

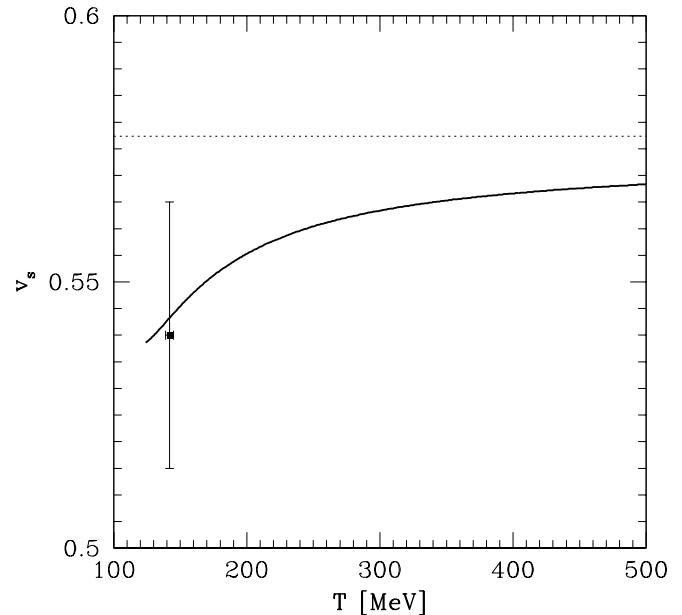


FIG. 9. The velocity of sound of quark-gluon liquid at $S/b = 42$. The dotted line corresponds to the value of the sound velocity of an ideal relativistic gas, $v_s = 1/\sqrt{3}$.

There is yet more evidence for the QGP nature of the fireball. It has been argued before that the values of the three other chemical parameters λ_s , γ_q and γ_s suggest as source a deconfined QGP fireball source [3]:

a) The value of strange quark fugacity λ_s can be obtained from the requirement that strangeness balances, $\langle N_s - N_{\bar{s}} \rangle = 0$, which for a source in which all s and \bar{s} quarks are unbound and thus have symmetric phase space, implies $\lambda_s = 1$. However, the Coulomb distortion of the strange quark phase space plays an important role in the understanding of this constraint for Pb-Pb collisions, leading to the Coulomb-deformed value $\lambda_s \simeq 1.1$, which is identical to the value obtained from experimental data analysis $\lambda_s^a = 1.09 \pm 0.02$.

b) The phase space occupancy of light quarks γ_q is, before gluon fragmentation, near or at the equilibrium value $\gamma_q = 1$. However, as measured by hadron abun-

dances it is expected to significantly exceed unity to accommodate the contribution from gluon fragmentation into light quark pairs. There is an upper limit: $\gamma_q < \gamma_q^c \equiv e^{m_\pi/2T_f} \simeq 1.67$, which arises to maximize the entropy density in the confined hadron phase.

c) The strange quark phase space occupancy γ_s can be computed within the framework of kinetic theory and is mainly influenced by strangeness pair production in gluon fusion [20], in early stages of the collision at high temperature, and by dilution effect in which the already produced strangeness over saturates the ‘thinner’ low temperature phase space. Moreover, some gluon fragmentation also enriches γ_s as measured by hadron abundance. We note that some earlier studies implicitly address the parameter γ_s/γ_q which therefore is stated in table I.

It is worthwhile to recall here that the strangeness yield, $s/b = \bar{s}/b \simeq 0.7$, predicted early on as the result of QGP formation [20] is also one of the results of data analysis seen in table I. This result is found with modern kinetic studies of strangeness production in QGP [3,4,24].

VI. DISCUSSION AND CONCLUSIONS

We have presented a detailed study of the interacting quark-gluon plasma equations of state, which have the property to reproduce precisely the latest lattice results for pressure and energy density. Since lattice results are obtained at vanishing baryon density, we must rely on theoretical behavior of the interacting quark-gluon gas when considering finite baryon density. This is done within the same computational approach in which the pressure and energy density are obtained correctly. Moreover, it turns out that the interaction correction is smallest for the baryon density, and thus, *a priori*, is most reliably described; however, its magnitude increases to the level of 45% at phase boundary. We also extrapolated to finite baryon density the interaction scale μ , as given in Eq.(3). Since there is arbitrariness of this extrapolation, we did check that, in the region of interest in the discussion of the SPS experimental data, the detail how the baryo-chemical potential is introduced into interaction scale does not matter: μ_b -contribution is in fact completely dominated by the T -contribution, since $(\pi T_c)^2 \simeq 50\mu_q^2$.

We have shown that the initial state of the QGP fireball, in pre-chemical equilibrium stage of light quarks, has been formed at about $T \simeq 270$ MeV, see figure 8. By the time, light quarks equilibrate temperature drops to just above $T \simeq 210$ MeV, and the energy density in such a QGP fireball is at $3 \text{ GeV}/\text{fm}^3$, as can be seen in figure 7, following the $S/b \simeq 42$ constrain back in time towards high temperature.

A significant change in the reaction mechanism can be expected when the opacity of the colliding nuclei is at or below 20%. Inspecting figure 8, we see that at that point,

formation of a deconfined phase is not assured considering where the boundary between hadrons and chemically non-equilibrated QGP is seen. This transparency certainly occurs for sufficiently small systems, where small is smaller than S–S, where stopping at the level of 35% is observed. On the other hand, results shown in figure 8 strongly suggest that the QGP-liquid phase should be formed at all energies accessible to SPS for Pb–Pb collisions. In fact, were it not for the uncertainties of extrapolation of lattice results to high baryon density, we would be rather certain that deconfinement also occurs in AGS energy range.

The results presented confirm in quantitative terms that the earlier non equilibrium analysis of hadron production is valid [3]. The non-equilibrium analysis method is more general than the equilibrium models [9], and it describes the hadron production data much better than competing approaches which assume quark chemical equilibrium conditions. This than introduces some doubts: because of the high precision of experimental data analysis, it was noted that the observed abundance of $\bar{\Omega}$ and Ω particles is above the yield pattern expected as established by other strange hadrons. The experimental $\bar{\Omega}$ excess we found is only 1.5 s.d.. However, the Ω excess is 5 s.d. and thus it seems that another production mechanism must contribute to this yield, beyond a purely statistical QGP fragmentation-recombination model. This effect becomes invisible under assumption of light quark equilibrium: higher particle yields are found at higher T_f [28], however the associated high value of the overall theory–experiment disagreement implies that some essential physical element is missing. When seeking to resolve this issue, we have found that the light quark pair abundance non equilibrium allows explanation of experimental data [5], with the usual 90% confidence level. This analysis result is found here to agree with the properties of the QGP-EoS which agree with the lattice-QCD results.

There were two objections to results of the non-equilibrium data analysis shown in table I:

a) The chemical freeze-out temperature T_f seemed to be too low, considering that the phase transition temperature has been estimated at about 170 MeV. However, we now have shown, see figure 5, that the low value $T_f = 143$ MeV is due to deep super-cooling of the rapidly expanding QGP, and there is a good agreement of our here presented findings about the phase transition in an equilibrium system with the consensus view about the properties of hot hadronic matter.

b) The light quark pair abundance fugacity (phase space occupancy) assumed a large value $\gamma_q \simeq 1.6$. Claim was made that there is no way that such strong nonequilibrium would not be directly visible in pion spectra and/or HBT analysis [26]. We have shown that features in pion spectra are in fact consistent with $\gamma_q \simeq 1.6$ [27], and it is now reported that HBT analysis is insensitive to γ_q . Thus, we believe that with the understanding of super-cooling effect [8], and the astounding agreement de-

scribed in section V between the QGP fireball properties and non-equilibrium data analysis results, this matter is settled in favor of the theoretically more palatable chemical non-equilibrium.

In conclusion, we have shown that equations of state of the quark-gluon liquid, fine tuned to exactly agree with the lattice results [6], are allowing a straightforward interpretation of the observed properties of the hadron fireball. We found that the energy per baryon and the entropy per baryon are agreeing with results of hadron production analysis, and that the velocity of expansion has the right magnitude and, as determined in data analysis, is just the sound velocity. Thus the quark-gluon liquid properties are found to be consistent with the observed physical properties of the fireball of dense hadronic matter formed in 158A GeV central Pb–Pb interactions at CERN.

It is important for the reader to appreciate that we did not fit any property of QGP to the experimental data, and that our comparison is based on EoS directly derived and extrapolated from the lattice-QCD results, using established expressions of thermal field theory. The main uncertainty in our procedure is that we use for the baryon density a purely theoretical result which, however, is obtained by the same thermal-QCD method as the pressure and energy (and entropy) which all agree with the lattice result once the two parameters, the scale $\mu(T)$ and vacuum energy \mathcal{B} , are fixed.

In our judgment, the good agreement we find between hadron abundance analysis and properties of lattice-EoS leave little, if any doubt that the SPS experiments involving Pb–Pb collisions at 158A GeV have reached the quark-gluon plasma phase of hadronic matter.

- [7] T. Csörgő, and L.P. Csernai, *Phys. Lett. B* **333**, 494 (1994).
- [8] J. Rafelski and J. Letessier “Sudden Hadronization in Relativistic Nuclear Collisions”, hep-ph/0006200.
- [9] T.S. Biró, “Quark Coalescence and Hadronic Equilibrium”, hep-ph/0005067.
- [10] J. Letessier, A. Tounsi and J. Rafelski, *Phys. Lett. B* **389**, 586 (1996).
- [11] S. Hamieh, J. Letessier, J. Rafelski, M. Schroedter and A. Tounsi, “Free Energy of a Hot Quark-Gluon Plasma”, hep-ph/0004016.
- [12] P. Arnold and C. Zhai, *Phys. Rev. D* **50**, 7603 (1994); **51**, 1906 (1995).
- [13] C. Zhai and B. Kastening, *Phys. Rev. D* **52**, 7232 (1995).
- [14] E. Braaten and A. Nieto, *Phys. Rev. Lett.* **76**, 1417, (1996); and *Phys. Rev. D* **53**, 3421 (1996).
- [15] J. Andersen, E. Braaten and M. Strickland, *Phys. Rev. Lett.* **83**, 2139, (1999); *Phys. Rev. D* **61**, 074016, (2000).
- [16] A. Peshier, B. Kämpfer and G. Soff, *Phys. Rev. C* **61**, 45203, (2000).
- [17] H. Vija and M.H. Thoma, *Phys. Lett. B* **342**, 212, (1995).
- [18] S.A. Chin, *Phys. Lett. B*, **78**, 552, (1978).
- [19] R. Hagedorn, *Suppl. Nuovo Cimento* **3**, 147 (1965); R. Hagedorn, Cargèse lectures in Physics, Vol. **6**, Gordon and Breach (New York 1977) and references therein; see also J. Letessier, H. Gutbrod and J. Rafelski, *Hot Hadronic Matter*, Plenum Press NATO-ASI series B346, New York (1995); H. Grote, R. Hagedorn and J. Ranft, “Atlas of Particle Production Spectra”, CERN black report (December 1970).
- [20] J. Rafelski and B. Müller, *Phys. Rev. Lett.* **48**, 1066 (1982); and **56**, 2334 (1986).
- [21] T. Biró, E. van Doorn, B. Müller, M.H. Thoma and X.-N. Wang, *Phys. Rev. C* **48**, 1275 (1993).
- [22] E. Shuryak, *Phys. Rev. Lett.*, **68**, 3270 (1992).
- [23] A. Bialas, *Phys. Lett. B* **466**, 301 (1999).
- [24] J. Rafelski, J. Letessier and A. Tounsi, *Acta Phys. Pol. B* **27**, 1035 (1996), and references therein.
- [25] R. Hagedorn and J. Rafelski *Phys. Lett. B* **97**, 136 (1980).
- [26] U. Heinz, *Nucl. Phys. A* **661**, 140c (1999).
- [27] J. Letessier, A. Tounsi and J. Rafelski, *Phys. Lett. B* **475**, 213 (2000).
- [28] J. Letessier, A. Tounsi and J. Rafelski, *Phys. Lett. B* **410**, 315 (1997).

* Supported in part by a grant from the U.S. Department of Energy, DE-FG03-95ER40937.

** LPTHE, Univ. Paris 6 et 7 is: Unité mixte de Recherche du CNRS, UMR7589.

- [1] <http://www.cern.ch/CERN/Announcements/2000/NewStateMatter>. Text of the scientific consensus view of the spokesmen of CERN experiments also available as: nucl-th/0002042, “Evidence for a New State of Matter: An Assessment of the Results from the CERN Lead Beam Program me”, compilation by U. Heinz and M. Jacob
- [2] J.C. Collins and M.J. Perry, *Phys. Rev. Lett.* **34**, 1353 (1975).
- [3] J. Letessier and J. Rafelski, “Observing Quark-Gluon Plasma with Strange Hadrons”, nucl-th/0003014, *Int. J. Mod. Phys. E* (2000) in press;
- [4] J. Letessier and J. Rafelski, *Acta Phys. Pol. B* **30**, 3559 (1999).
- [5] J. Letessier, and J. Rafelski, *J. Phys. G* **25**, 295 (1998); *Phys. Rev. C* **59**, 947 (1999).
- [6] F. Karsch, E. Laermann and A. Peikert, *Phys. Lett. B* 478, 447-455, (2000).